ISSN 1054-660X, Laser Physics, 2012, Vol. 22, No. 1, pp. 216–220.

Generation of Optical Waveforms in 1.3-μm SOA-Based Fiber Lasers[1]

J.-Y. Wang[a], K.-H. Lin[a, *], and H.-R. Chen[b]

[a] *Department of Science, Taipei Municipal University of Education, 1, Ai-Kuo West Road, Taipei 100, Taiwan*
[b] *Department of Photonics and Institute of Electro-Optical Engineering, National Chiao Tung University, 1001, Ta-Hsueh Road, Hsinchu 300, Taiwan*
*e-mail: khlin@tmue.edu.tw

Received June 19, 2011; in final form, June 29, 2011; published online October 24, 2011

Abstract—Passive optical waveform generation is obtained in fiber lasers using a 1.3-μm semiconductor optical amplifier (SOA) as the gain medium. Various waveforms, including square wave, staircase wave, triangular wave, pulse, and dark pulse are generated in SOA-based fiber lasers by adjusting intracavity polarization controllers. The passive waveform generation might be attributed to the SOA gain dynamics and the enhanced nonlinear interaction at the 1.3-μm zero dispersion wavelength of traditional single-mode fiber (SMF), as well as the interference effect between the two sub-cavities of fiber laser. With figure-8 cavity configuration, 1250th-order harmonic pulses have been successfully demonstrated. We have also obtained a free-running SOA-based fiber laser with 3-dB spectral width of 16 nm, and the center wavelength can be tuned over 45 nm range.

DOI: 10.1134/S1054660X11230198

1. INTRODUCTION

Many rare-earth-doped fibers have been used as the active media of fiber lasers [1]. Among these active media, erbium-doped fibers (EDFs) and ytterbium-doped fibers (YDFs) have attracted much attention in the construction of either continuous-wave (CW) or pulsed fiber lasers [2–5]. Recently, semiconductor optical amplifiers (SOAs) provide interesting alternatives as the gain media in fiber laser cavities because of their dominant inhomogeneous broadening properties and the ease of integration with other devices [6–17]. As compared to the rare-earth-doped fibers, SOAs can generate multiple stable lasing wavelengths at room temperature, which make them attractive for applications in telecommunication systems and photonic technologies [18, 19]. Pleros et al. demonstrated multi-wavelength and power-equalized operation in a 1.55-μm SOA-based ring laser that uses a fiber Fabry–Perot filter [6]. Simultaneous oscillation of 52 lines with 50-GHz spacing is achieved by using single-pass optical feedback. Multi-wavelength fiber lasers can also be obtained by incorporating fiber Bragg gratings (FBGs) or arrayed waveguide gratings (AWGs) in the SOA-based cavity [11–13]. Latif et al. presented the design of a quad-wavelength fiber laser that covers the 1.3- and 1.55-μm bands using two SOAs and an AWG of 100-GHz interchannel spacing [13]. Their design is capable of providing more than 24 ways of tuning the wavelength spacings. A recently proposed scheme of SOA-based fiber laser adopted a Sagnac loop mirror (SLM) in the cavity to generate multiple lasing lines [20, 21]. Using this scheme, Zulkifli et al. [20] have obtained 60 wavelengths oscillating simultaneously between 1464 and 1521 nm with a spacing of 0.92 nm.

Pulse generation in a fiber laser may employ either active or passive technology [22–24]. Using a intracavity Mach-Zehnder intensity modulator, Tang et al. have generated tunable picosecond pulses from a 10-GHz harmonically mode-locked SOA ring laser with a center wavelength spanning from 1491 to 1588 nm [16]. In order to generate ultrashort pulses in fiber lasers, passive mode-locking (PML) have been widely reported based on several types of mechanisms. Due to its long cavity length, significant interactions between dispersive and dissipative optical effects, such as Kerr nonlinearity, chromatic dispersion, linear and saturable losses, as well as bandwidth-limited gain, can be experienced in a fiber laser even under moderate pump powers. Yang et al. reported the generation of sub-picosecond optical pulses using an SOA and a linear polarizer in a ring laser cavity [10]. For this laser, nonlinear polarization rotation in the SOA serves as the passive mode-locking mechanism. By using a figure-8 fiber laser cavity, nonlinear amplification can also be designed to favor mode-locking [1, 15].

Passively mode-locked short pulse lasers often contain two main elements: (a) a gain medium that is responsible for the amplification of the pulse, and (b) a nonlinear optical device that is responsible for the compression of the pulse. Using nonlinear polarization evolution (NPE) technology for pulse generation has avoided the use of saturable absorber and thus simplifies the cavity configuration. NPE mode-locking has been utilized in erbium-doped fiber lasers

[1] The article is published in the original.

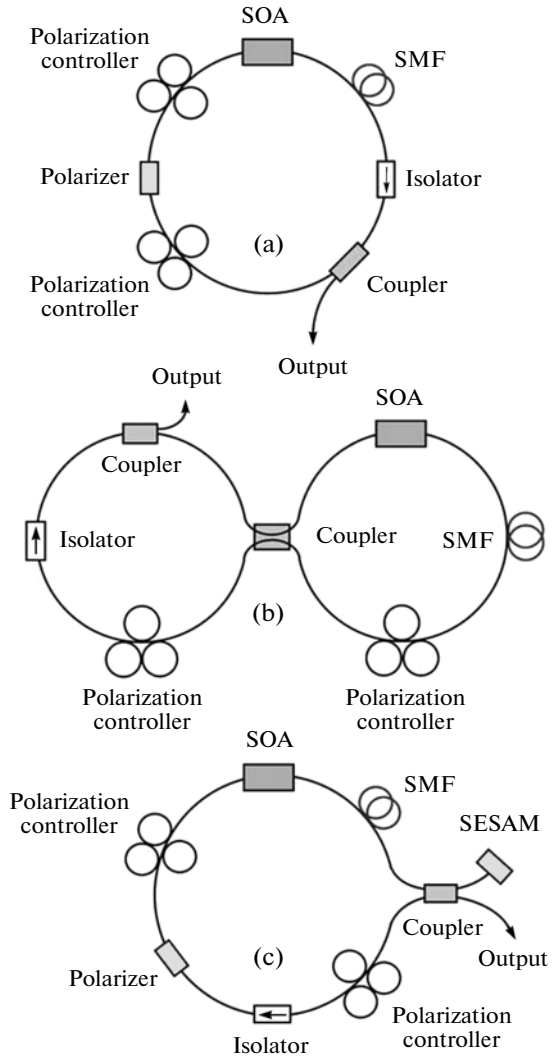

Fig. 1. Experimental setup of SOA fiber lasers: (a) a conventional NPE ring cavity, (b) a figure-8 cavity, and (c) a σ-cavity SOA fiber laser with semiconductor saturable absorber mirror.

(EDFLs) and ytterbium-doped fiber lasers (YDFLs) to generated femtosecond light pulses [3, 25, 26]. However, the waveforms of these passively mode-locked fiber lasers are governed by the Ginzburg-Landau equation and the commonly observed pulse shapes are $sech^2$, Gaussian, or parabolic. For anomalous dispersion lasers, soliton formation is mainly attributed to the interplay between the anomalous cavity dispersion and the self-phase modulation effect. For normal dispersion lasers, however, soliton formation is resulted from the interaction between normal dispersion and intracavity bandwidth filtering. Wu et al. have reported the generation of square-profile dissipative solitons from an all-normal-dispersion erbium-doped fiber laser which is mode-locked with the nonlinear polarization rotation technique [27].

It is interesting to raise a question now: what kind of pulses will be generated in the zero or nearly zero dispersion fiber lasers? In fact, generation and shaping of optical pulses in the 1.3-μm regime are rarely reported for SOA-based fiber lasers, despite the enhanced wave-mixing effect in the SOA gain medium as well as the zero-dispersion regime of conventional single-mode fibers. As inspired by the electronic waveform generators, an optical counterpart capable of providing square wave, sinusoidal wave, and triangular wave, etc., is attractive for applications in optical communication, signal processing, and device characterization. In this work we present a passive technology for optical waveform generation by using 1.3-μm SOA-based fiber lasers. Various waveforms such as square wave, staircase wave, triangular wave, pulse, and dark pulse have been successfully generated with proper cavity design and the adjustment of intracavity polarization.

2. EXPERIMENTAL SETUP

Figure 1 shows the experimental setup of the SOA-based fiber lasers. In our experiment, we have adopted three cavity configurations: (1) a conventional NPE ring cavity (Fig. 1a), (2) a figure-8 cavity (Fig. 1b), and (3) a σ cavity with the insertion of a semiconductor saturable absorber mirror (SESAM) (Fig. 1c). The SOA has a peak output wavelength of 1290 nm and 3-dB bandwidth of 54 nm; the maximum small signal gain is 20.9 dB and the saturation output power is 10.8 dBm (measured from the output port). Since SOA is a bi-directional device, an optical isolator is used in the cavity to ensure unidirectional laser oscillation. A roll of 2-km single-mode fiber (SMF) is inserted in the cavity to enhance the interaction length. The output coupling is 10% for the ring and figure-8 cavities, while it is 50% for the σ cavity. Almost all the fiber components in the laser cavity are linked via single-mode-fiber jumpers with FC/APC connectors, except that the SOA connections are FC/PC.

For the NPE cavity, the combination of polarizer and polarization controllers works effectively as the nonlinear loss. For the figure-8 cavity, a 3-dB coupler is used to connect the two fiber loops. The sub-cavity containing the SOA works effectively as nonlinear gain. The laser operation states are monitored by using a high-speed InGaAs photodetector and a digital oscilloscope (HP 54542C), while the output spectra is recorded by an optical spectrum analyzer (Agilent 86146B). A power meter (Thorlabs Inc.) and a radio frequency (RF) spectrum analyzer (HP 8560E) are used to measure the output power and the longitudinal mode beating.

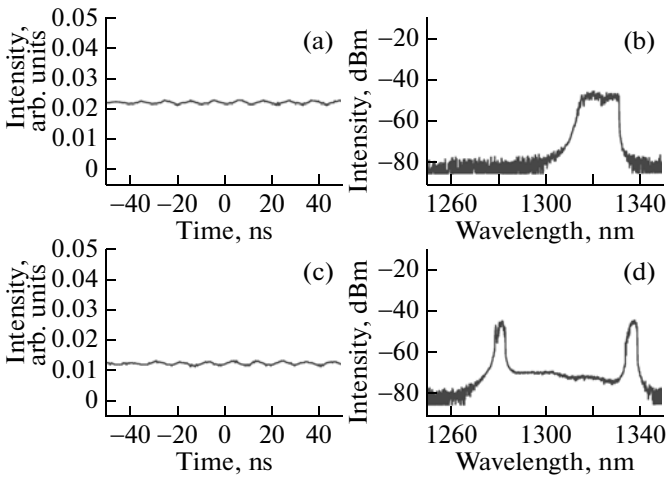

Fig. 2. Oscilloscope traces and optical spectra for the ring-cavity SOA laser. (a) and (b): single-band operation with center wavelength of 1324 nm and 3-dB spectral width of 16 nm; (c) and (d): dual-band operation with wavelength spacing of 56 nm.

3. RESULTS AND DISCUSSIONS

Initially we have adopted the conventional NPE laser cavity of 10% output coupling (Fig. 1a). The SOA current is set to 240 mA. By adjusting the polarization controllers, the laser can be operated in the free-running state with single, dual, or even 3 to 4 spectral bands. We have obtained a single-band SOA fiber laser with center wavelength of 1324 nm and 3-dB spectral width of 16 nm (Figs. 2a and 2b), and the laser output power is –0.2 dBm. The center wavelength of single-band operation can be tuned over 45 nm range. By further adjustment of the polarization controllers, we have obtained dual-band laser operation with wavelength spacing of 56 nm (Figs. 2c and 2d), but the output power is decreased to –2.8 dBm and the spectral width of each band is reduced. We have carefully adjusted the two polarization controllers in Fig. 1a, but the laser still works in the free-running mode without any pulse generation.

It is interesting that a free-running laser can provide spectral width as large as 16 nm, since the maximum intracavity power of our SOA-based fiber laser is only about 10 mW. Although the bandwidth of oscilloscope is 500 MHz and the sampling rate is 2 Gb/s, we have used a 2.9-GHz RF spectrum analyzer (HP 8560E) to monitor the laser output, and still we do not observe pulse signals. Therefore, the broad laser spectrum might be a result of inhomogeneous broadening instead of mode-locking. When the 2-km single mode fiber is removed from the cavity, the laser spectrum shows some minor dips with 1.4 nm spacing, which should be attributed to the residual reflections from the SOA surfaces and the accompanying parasitic Fabry–Perot modes. The spectral dips are eliminated when the 2-km SMF is inserted in the cavity, which should be attributed to the spectral broadening effect inside the long intracavity fiber.

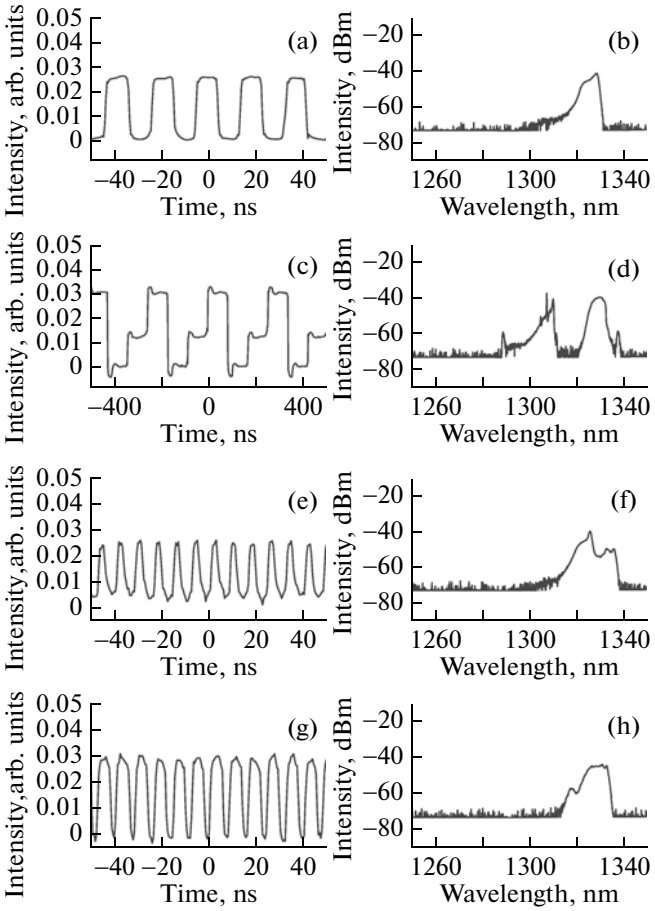

Fig. 3. Optical waveforms and spectra generated in the figure-8 cavity with the insertion of 2-km SMF. (a) and (b): square wave; (c) and (d): staircase wave; (e) and (f): pulse; (g) and (h): dark pulse.

However, with the figure-8 cavity configuration (Fig. 1b), various optical waveforms have been successfully generated with careful polarization tuning. Figures 3a, 3c, 3e, 3g show the observed pulse trains of square wave, staircase wave, pulse, and dark pulse, while the corresponding output spectra are shown in Figs. 3b, 3d, 3f, 3h, respectively. The table summarizes the characteristics for these optical waveforms generated in the figure-8 cavity. The pulse separation for

Characteristics of optical waveforms in figure 8 SOA-based fiber laser cavity with 2-km SMF

Waveform	Output Power, dBm	Repetition Rate, MHz
Square	2.6	50
Staircase	2.6	4
Pulse	2.1	125
Dark Pulse	3.9	125

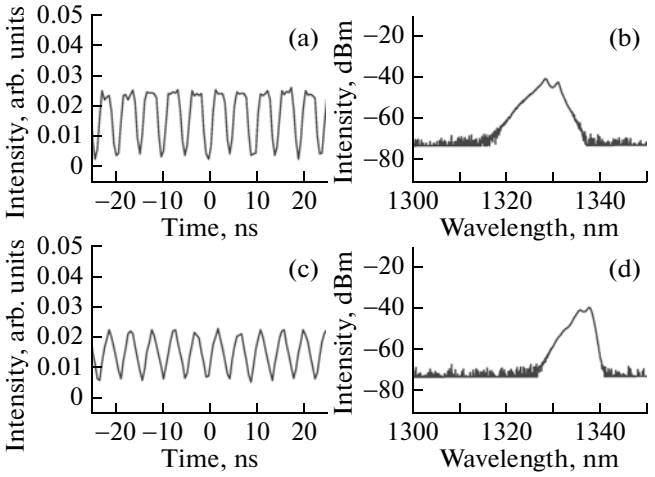

Fig. 4. Optical waveforms and spectra generated in the figure-8 cavity without the 2-km SMF. (a) and (b): dark pulse; (c) and (d): triangular wave.

square wave is 20 ns (Fig. 3a), and the laser output power is 2.6 dBm. For staircase wave, the output power is also 2.6 dBm, but the pulse spacing is increased to 250 ns (Fig. 3c). Some overshoots are observed on the rising edges of staircase wave. Depending on the polarization adjustment, the staircase wave could either be upstairs or downstairs. By further adjustment of the polarization controllers, the optical waveform can be switched to pulse or dark pulse. Figures 3e and 3g shows the oscilloscope trace for pulses and dark pulses, respectively. The pulse shape resembles that of solitons, while the dark pulse looks like dark solitons. Both of them have pulse separations of 8 ns, but the output powers are 2.1 and 3.9 dBm for pulse and dark pulse states. The output spectra show single band around 1325 nm for square wave, pulse, and dark pulse states. However, dual-band spectrum is observed for the staircase wace.

With a 2-km figure-8 cavity, the round-trip time is about 10 μs and the pulse repetition rate is about 100 kHz; however, we have not observed this fundamental pulse trains, although the intracavity power is only moderate (≈10 mW). The lowest-order pulse repetition rate achieved is 4 MHz for the staircase wave, corresponding to 40th-order harmonics. For pulse and dark pulse trains, the repetition rate is 125 MHz, which corresponds to 1250th-order harmonic pulse generation. As a comparison, it is easier for rare-earth-doped fiber lasers, such as erbium-doped and ytterbium-doped fiber lasers, to operate in fundamental mode-locking states than harmonic mode-locking states under such low intracavity powers.

When the 2-km SMF is removed from the figure-8 cavity, dark pulses can be obtained with 5-ns spacing (Fig. 4a), and the output power is 3.6 dBm. The output spectrum shows a single-band structure, and the peak wavelength is located at about 1328 nm (Fig. 4b). By

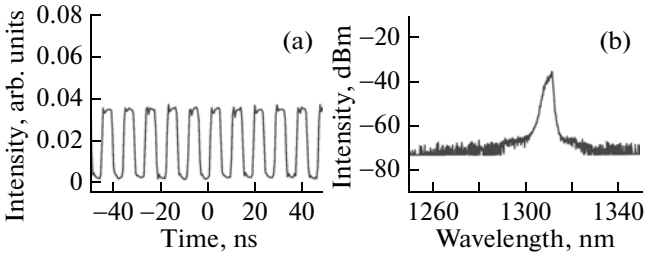

Fig. 5. (a) Oscilloscope trace and (b) optical spectrum for the σ-cavity SOA fiber laser.

tuning the polarization controllers, triangular pulses have be generated (Fig. 4c). The pulse spacing is also 5 ns for triangular wave and the output power is somewhat reduced to 3.3 dBm. Again the spectrum shows a single-band structure, but the peak wavelength is shift to about 1335 nm (Fig. 4d). It seems that the triangular wave is a transition state from pulse state to dark-pulse state.

The passive waveform generation might be attributed to the SOA gain dynamics and the enhanced nonlinear interaction at the 1.3-μm zero dispersion wavelength of SMF, as well as the interference effect between the two sub-cavities of figure-8 laser. In addition, it seems easier to generate optical waveforms in a coupled cavity than a single-ring cavity. We have demonstrated this by using a σ-cavity SOA fiber laser, where a semiconductor saturable absorber mirror is connected to the main cavity by a 2 × 2 3-dB coupler, as shown in Fig. 1c. The SESAM in the σ cavity is originally designed for the 1550-nm band (Batop, SAM 1550-23-2ps-FC/APC). It has an unsaturated absorption of $A_0 = 23\%$ and modulation depth of $\Delta R = 14\%$ at 1550 nm, with saturation fluence of 25 μJ/cm^2.

For the σ-cavity SOA-based fiber laser, we find that the square-wave pulses can also be generated by adjusting the polarization controllers. Figure 5a shows the laser output signals observed on the oscilloscope, and the corresponding optical spectrum is shown in Fig. 5b. The oscilloscope trace demonstrates a train of square waves with pulse spacing of 10 ns, while the center wavelength of these pulses is 1310 nm. Since the laser wavelength is far from the operating wavelength (1550 nm) of this SESAM, passive waveform generation might be attributed to coupling effect provided by the back reflection from the SESAM as well as the enhanced nonlinear interaction at the zero dispersion wavelength of conventional single-mode fiber.

4. CONCLUSIONS

We have developed a passive technology to generate optical waveforms by using a 1.3-μm SOA-based fiber laser. Various waveforms such as square wave, staircase wave, triangular wave, pulse, and dark pulse have been successfully generated with proper cavity design and

the adjustment of intracavity polarization. Harmonic pulses as high as 1250th-order has been generated with a figure-8 laser configuration, although the intracavity power is only at moderate level of about 10 mW. The passive optical waveform generation might be attributed to the nonlinear interaction in single-mode fiber and the SOA gain dynamics, as well as the wave coupling effect between sub-cavities. Passive generation of optical waveforms may potentially be used in optical function generators as well as applications in optical communication, signal processing, and device characterization in the future.

ACKNOWLEDGMENTS

This work is supported partially by the National Science Council of Taiwan, Republic of China, under grant NSC99-2221-E-133-001.

REFERENCES

1. G. P. Agrawal, *Applications of Nonlinear Fiber Optics* (Academic Press, 2008), ch. 5.
2. O. Okhotnikov, A. Grudinin, and M. Pessa, New J. Phys. **6**, 177 (2004).
3. M. E. Fermann and I. Hartl, IEEE J. Sel. Top. Quantum Electron. **15**, 191 (2009).
4. K.-H. Lin, J.-J. Kang, H.-H. Wu, C.-K. Lee, and G.-R. Lin, Opt. Express **17**, 4806 (2009).
5. K.-H. Lin, J.-H. Lin, and C.-C. Chen, Laser Phys. **20**, 1984 (2010).
6. N. Pleros, C. Bintjas, M. Kalyvas, G. Theophilopoulos, K. Yiannopoulos, S. Sygletos, and H. Avramopoulos, IEEE Photon. Technol. Lett. **14**, 693 (2002).
7. A. A. Moiseev, G. V. Gelikonov, E. A. Mashcovitch, and V. M. Gelikonov, Laser Phys. Lett. **7**, 505 (2010).
8. H. Ahmad, M. Z. Zulkifli, A. A. Latif, and S. W. Harun, Laser Phys. Lett. **7**, 164 (2010).
9. V. Baby, L. R. Chen, S. Doucet, and S. LaRochelle, IEEE J. Sel. Top. Quantum Electron. **13**, 764 (2007).
10. X. Yang, Z. Li, E. Tangdiongga, D. Lenstra, G. D. Khoe, and H. J. S. Dorren, Opt. Express **12**, 2448 (2004).
11. H. Ahmad, A. H. Sulaiman, S. Shahi, and S. W. Harun, Laser Phys. **19**, 1002 (2009).
12. Y. Wei and B. Sun, Laser Phys. **19**, 1252 (2009).
13. A. A. Latif, M. Z. Zulkifli, N. A. Hassan, S. W. Harun, Z. A. Ghani, and H. Ahmad, Laser Phys. Lett. **7**, 597 (2010).
14. Z. Li, X. Yang, E. Tangdiongga, H. Ju, G.-D. Khoe, H. J. S. Dorren, and D. Lenstra, IEEE J. Quantum Electron. **41**, 808 (2005).
15. Y. H. Zhong, Z. X. Zhang, and X. Y. Tao, Laser Phys. **20**, 1756 (2010).
16. W. W. Tang, M. P. Fok, and Ch. Shu, Opt. Express **14**, 2158 (2006).
17. F. M. Wu, P. C. Peng, J. Chen, C. T. Lin, and W. C. Kao, Laser Phys. **21**, 522 (2011).
18. H. Ahmad, K. Thambiratnam, A. H. Sulaiman, N. Tamchek, and S. W. Harun, Laser Phys. Lett. **5**, 726 (2008).
19. H. Ahmad, M. Z. Zulkifli, K. Thambiratnam, A. A. Latiff, and S. W. Harun, Laser Phys. Lett. **6**, 539 (2009).
20. M. Z. Zulkifli, N. A. Hassan, N. A. Awang, Z. A. Ghani, S. W. Harun, and H. Ahmad, Laser Phys. Lett. **7**, 673 (2010).
21. J. E. Im, B. K. Kim, and Y. Chung, Laser Phys. **20**, 1918 (2010).
22. M. Hofer, M. E. Fermann, F. Haberl, M. H. Ober, and A. J. Schmidt, Opt. Lett. **16**, 502 (1991).
23. J. Fekete, A. Cserteg, and R. Szipocs, Laser Phys. Lett. **6**, 49 (2009).
24. Y. J. Song, M. L. Hu, C. L. Gu, L. Chai, C. Y. Wang, and A. M. Zheltikov, Laser Phys. Lett. **7**, 230 (2010).
25. F. W. Wise, A. Chong, and W. H. Renninger, Laser Photon. Rev. **2**, 58 (2008).
26. J.-H. Lin, D. Wang, and K.-H. Lin, Laser Phys. Lett. **8**, 66 (2011).
27. X. Wu, D. Y. Tang, H. Zhang, and L. M. Zhao, Opt. Express **14**, 5580 (2009).